





MicroRNA-92b-3p is a prognostic oncomiR that targets *TSC1* in clear cell renal cell carcinoma

Cong Wang¹  | Motohide Uemura^{1,2} | Eisuke Tomiyama¹ | Makoto Matsushita¹ | Yoko Koh¹ | Kosuke Nakano¹ | Yujiro Hayashi¹  | Yu Ishizuya¹ | Kentaro Jingushi³ | Taigo Kato^{1,2}  | Koji Hatano¹ | Atsunari Kawashima¹  | Takeshi Ujike¹ | Akira Nagahara¹ | Kazutoshi Fujita¹ | Ryoichi Imamura¹ | Kazutake Tsujikawa³ | Norio Nonomura¹

¹Department of Urology, Osaka University Graduate School of Medicine, Suita, Japan

²Department of Urological Immuno-Oncology, Osaka University Graduate School of Medicine, Suita, Japan

³Laboratory of Molecular and Cellular Physiology, Osaka University Graduate School of Pharmaceutical Sciences, Suita, Japan

Correspondence

Motohide Uemura, Department of Urology, Osaka University Graduate School of Medicine, Suita, Japan.
Email: uemura@uro.med.osaka-u.ac.jp

Funding information

Japan Society for the Promotion of Science, Grant/Award Number: Grant number: A16H069540

Abstract

Although several studies have reported that microRNA (miR)-92b-3p is involved in various cellular processes related to carcinogenesis, its physiological role in clear cell renal cell carcinoma (ccRCC) remains unclear. To clarify the role of miR-92b-3p in ccRCC, we compared miR-92b-3p expression levels in ccRCC tissues and adjacent normal renal tissues. Significant upregulation of miR-92b-3p was observed in ccRCC tissues. Overexpression of miR-92b-3p using a miRNA mimic promoted proliferation, migration, and invasion activities of ACHN cells. Functional inhibition of miR-92b-3p by a hairpin miRNA inhibitor suppressed Caki-2 cell growth and invasion activities *in vitro*. Mechanistically, it was found that miR-92b-3p directly targeted the *TSC1* gene, a known upstream regulator of mTOR. Overexpression of miR-92b-3p decreased the protein expression of *TSC1* and enhanced the downstream phosphorylation of p70S6 kinase, suggesting that the mTOR signaling pathway was activated by miR-92b-3p in RCC cells. Importantly, a multivariate Cox proportion hazard model, based on TNM staging and high levels of miR-92b-3p, revealed that miR-92b-3p expression (high vs. low hazard ratio, 2.86; 95% confidence interval, 1.20-6.83; $P = .018$) was a significant prognostic factor for overall survival of ccRCC patients with surgical management. Taken together, miR-92b-3p was found to act as an oncomiR, promoting cell proliferation by downregulating *TSC1* in ccRCC.

KEYWORDS

ccRCC, miR-92b-3p, oncomiR, proliferation, *TSC1*

Abbreviations: ccRCC, clear cell renal cell carcinoma; CI, confidence interval; HR, hazard ratio; miR, microRNA; oncomiR, oncogenic microRNA; OS, overall survival; RCC, renal cell carcinoma; S6K, p70 ribosomal S6 kinase β -1; TCGA, The Cancer Genome Atlas; *TSC1*, TSC complex subunit 1.

This is an open access article under the terms of the Creative Commons Attribution-NonCommercial-NoDerivs License, which permits use and distribution in any medium, provided the original work is properly cited, the use is non-commercial and no modifications or adaptations are made.

© 2020 The Authors. *Cancer Science* published by John Wiley & Sons Australia, Ltd on behalf of Japanese Cancer Association.

1 | INTRODUCTION

The incidence and mortality of RCC have been increasing in recent years in Japan.¹ Among all RCC cases, approximately 70% to 80% of subtypes are ccRCC. Approximately 20%-30% of RCC patients have metastatic disease at the time of diagnosis, and 20%-40% develop metastases later after nephrectomy.² There are no early detection or prognostic biomarkers in routine clinical practice, and the mechanisms involved in RCC development and progression remain unclear. Hence, understanding the molecular mechanisms involved in the pathogenesis of RCC is crucial for developing new cancer prevention strategies.

MicroRNAs are noncoding RNAs that regulate gene expression, mainly at the translational level.³ Anomalous changes in miRNA expression have been reported in several human cancers and are associated with tumorigenesis.⁴⁻⁶ In our previous microarray analysis, we identified several miRNAs that were significantly overexpressed in ccRCC and that were thought to be involved in proliferation, migration, and invasion.⁷⁻⁹ However, none of them were found to be associated with long-term OS in ccRCC patients.

MicroRNA-92b-3p is one of the upregulated miRNAs in ccRCC tissues, according to our previous study,⁹ and it has been revealed as an oncomiR in colorectal carcinoma¹⁰ and gastric cancer.¹¹ In contrast, miR-92b-3p might also function as a tumor suppressor RNA in pancreatic cancer.¹² Hence, the physiological role of miR-92b-3p varies according to the types of cancer, and the precise mechanism of miR-92b-3p in ccRCC progression remains unknown.

In this study, we undertook a functional analysis of miR-92b-3p in RCC cells and evaluated the association of upregulated miR-92b-3p with prognosis in ccRCC patients. Our data showed for the first time that miR-92b-3p functions as an oncomiR by regulating *TSC1* as the direct target gene in RCC cell lines and influences cell proliferation by regulating the *TSC1*-mTOR signaling pathway. Collectively, our findings suggest that miR-92b-3p is a promising target for RCC treatment and a potential prognostic marker in ccRCC.

2 | MATERIAL AND METHODS

2.1 | Chemicals and Abs

Monoclonal anti-TSC1 Ab was purchased from Thermo Fisher Scientific (clone: 5C8A12, #37-0400). Monoclonal anti-phospho-p70 S6 kinase (Thr³⁸⁹) Ab (clone: 108D2, #9234) and polyclonal anti-p70 S6 kinase Ab (#9202) were purchased from Cell Signaling Technology. Monoclonal anti- β -actin Ab was purchased from Sigma (clone: AC-74). miRIDIAN miRNA hairpin inhibitor negative control, miRIDIAN miRNA mimic negative control, miRIDIAN hairpin inhibitor, and miRIDIAN miRNA mimic for human hsa-miR-92b-3p (MIMAT0003218) were purchased from Horizon Dharmacon.

2.2 | Clinical specimens

Clear cell RCC specimens were obtained from patients while they underwent primary resection at Osaka University Hospital from July 2002 to August 2010. Tumor-associated normal renal tissue was also obtained from a subset of these patients when possible. Written informed consent was obtained from all patients, and the study was approved by the ethics committee of Osaka University Hospital (#13397-2 and #14069-3). Tumor stage was determined according to the 6th edition of the American Joint Committee on Cancer stage classification,¹³ and grading was determined according to the International Histological Classification of Tumours.¹⁴ Clinical characteristics of the patients related to these samples are presented in Tables 1 and 2.

2.3 | Quantitative real-time PCR

Following excision, tissue samples were immediately immersed in RNeasy lysis buffer (Qiagen) and stored at -20°C until RNA extraction. MicroRNAs were purified using the miRNeasy mini kit according to manufacturer's instructions (Qiagen). Real-time PCR analysis was undertaken to validate the miR-92b-3p expression in 20 matched-pair samples and 75 tumor samples of ccRCC using the Mir-X miRNA first-strand synthesis kit (Takara). Thermal cycling conditions included an initial step at 98°C for 30 seconds, and 40 cycles at 95°C for 2 seconds and 63°C for 5 seconds using a miR-92b-3p-specific primer (5'-tattgcactcgtcccggcctcc-3') and a U6 snRNA primer (Takara) as an internal control. Total RNA was isolated by using TRIzol reagent (Invitrogen). The PrimeScript RT reagent Kit (Takara) was used to prepare cDNA from 500 ng total

TABLE 1 Clinical characteristics of 20 patients with clear cell renal cell carcinoma for real-time PCR analysis (validation of microRNA-92b-3p expression)

Age, median years (range)	57 (37-84)
Gender	
Male	14
Female	6
Histological type	
Clear cell	20
Grade (highest)	
G1	3
G2	11
G3	6
Pathological T stage	
1a	11
1b	3
2a	2
3a	2
3b	1
3c	1

TABLE 2 Clinical characteristics of patients with clear cell renal cell carcinoma for overall survival analysis (n = 75)

Age, median years (range)	64 (39-82)
Gender	
Male	48
Female	27
Histological type	
Clear cell	75
TNM Stage	
I	29
II	16
III	18
IV	12
Grade (highest)	
G1	6
G2	51
G3	18
Vascular invasion	
Yes	18
No	55
N/A	2
NLR, median (range)	2.52 (0.89-14.69)
PLR, median (range)	1.48 (0.57-5.37)
CRP, median mg/dl (range)	0.20 (0.04-17.20)
Serum sodium concentration, median mEq/L (range)	140 (134-144)
Follow-up time, median months (range)	100 (0.00-195)

Abbreviations: CRP, C-reactive protein; N/A, not available; NLR, neutrophil to lymphocyte ratio; PLR, platelet to lymphocyte ratio.

RNA. Both mRNA expression and miRNA expression were quantified as delta Ct values.

2.4 | Cell culture

Four human ccRCC cell lines (786-O, Caki-1, Caki-2, and ACHN), obtained from the ATCC, were cultured in RPMI-1640 medium (Wako) supplemented with 10% FBS, 100 U/mL penicillin G, and 0.1 µg/mL streptomycin.

2.5 | Western blot analyses

Cells were lysed with Laemmli SDS sample buffer (Bio-Rad) containing 5% 2-mercaptoethanol. Protein samples were separated on a 7.5%-15% SDS-PAGE gel and then transferred to a PVDF membrane using the Bio-Rad semidry transfer system (1 hour, 12 V). Immunoreactive proteins made to react with the Abs described previously were visualized by treatment with an ECL Prime Western blotting detection reagent (GE Healthcare).

2.6 | MicroRNA hairpin inhibitor, mimic transfection

miRIDIAN miRNA hairpin mimics, hairpin inhibitors, and mimic/inhibitor negative controls were transfected at a concentration of 50 nmol/L using Lipofectamine RNAiMAX reagent (Thermo Fisher Scientific).

2.7 | Luciferase reporter assay

A pmirGLO dual-luciferase miRNA target expression vector was used for the 3'-UTR luciferase reporter assay (Promega). The following sequences of oligos were used for the construction of the pmirGLO/TSC1 3'-UTR vector:

5'-ctagcgccgctagtggttgctccttgaacctgtcaatag-3' and 5'-tcgactattgcacaggttcaaaggacgcaaccactagcggccgctagagct-3'.

ACHN cells were cotransfected with 50 nmol/L miR-92b-3p (or control mimic) and luciferase reporter constructs, and Caki-2 cells were cotransfected with 50 nmol/L miR-92b-3p (or control inhibitor) and luciferase reporter constructs using Lipofectamine 2000 (Thermo Fisher Scientific). Forty-eight hours later, luciferase assays were carried out, and luciferase activity was determined using a Turner Biosystems 20/20 luminometer (Promega) with a microplate reader (Bio-Rad).

2.8 | Cell growth assay

ACHN or Caki-2 cells transfected with miRIDIAN hairpin inhibitor or mimic were reseeded in 96-well plates (5×10^2 cells/100 µL) and incubated for the indicated time. Twenty microliters of CellTiter 96 Aqueous One Solution Reagent (Promega) were added and incubated at 37°C and 5% CO₂ (Caki-2 cells, 1.5 hours; ACHN cells, 2.5 hours). The absorbance at 490 nm was measured with a microplate reader (Bio-Rad).

2.9 | Wound healing assay

Cell migration was evaluated using wound healing assays. Caki-2 or ACHN cells transfected with the miRIDIAN hairpin inhibitor or mimic were seeded in a 24-well plate (Caki-2 cells, 2.0×10^4 cells/well; ACHN, 1.0×10^4 cells/well) and incubated for 72 hours. A wound was created in a monolayer of each line using a sterile 1-mL pipette tip at approximately 90% confluence, and cell pictures were recorded at 0 and 18 hours for both Caki-2 and ACHN cells after wound creation.

2.10 | Cell invasion assay

Invasion assays were undertaken using the BD BioCoat Matrigel Invasion Chamber (pore size 8 µm) (Becton Dickinson). Caki-2 cells

or ACHN cells transfected with the miRIDIAN hairpin or mimic for 72 hours were reseeded into the inserts of 24-well plates (Caki-2 cells, 2.0×10^4 cells/well; ACHN, 1.5×10^4 cells/well) in serum-free media, with the base plate containing RPMI supplemented with 10% FBS. After 48 hours of incubation at 37°C, cells that had penetrated the Matrigel were fixed and stained using Diff-Quik stain (Sysmex).

2.11 | Everolimus treatment

ACHN cells transfected with the miR-92b-3p mimic or a negative control miRNA mimic for 24 hours were reseeded in a 96-well plate and incubated for another 24 hours. Subsequently, 100 nmol/L everolimus (RAD001) (ChemScene) or a vehicle (0.1% DMSO) was added to the transfected ACHN cells for 96 hours, then cell viability was examined by MTS assay.

2.12 | Immunohistochemistry

The expression of TSC1 was determined by immunohistochemical staining of paraffin-embedded tissues of ccRCC samples alongside healthy counterparts. Formalin-fixed paraffin-embedded sections (4 μ m in thickness) were deparaffinized and rehydrated. After the slides were steamed for 20 minutes in 10 mmol/L citrate buffer (pH 6.0) for antigen retrieval, endogenous peroxidase was blocked using 3% H₂O₂. Immunohistochemical staining for TSC1 was carried out using anti-TSC1 Ab (clone: 5C8A12, #37-0400; Thermo Fisher Scientific) and the EnVision+ Detection System (Dako) according to the manufacturer's instructions. Primary Ab was incubated overnight at 4°C and counterstained with hematoxylin.

The levels of TSC1 staining were classified into 2 groups according to the staining intensity of the positive cells (staining score, 1-2).

2.13 | Survival analysis

Clear cell RCC patients from the TCGA cohort were used to assess the correlation between miR-92b-3p expression and OS. The prognostic data and Kaplan-Meier curve were calculated using the SurvMicro web tool (<http://bioinformatica.mty.itesm.mx:8080/Biomatec/Survmicro.jsp>). Patients were divided into 2 groups (high- and low-risk group), according to the prognostic index calculated by multivariate survival analysis using a Cox regression model.

2.14 | Statistics

Results are expressed as the mean \pm SD, and values were compared using the Mann-Whitney *U* test or unpaired Student's *t* test. Overall survival was analyzed using the Kaplan-Meier method, and differences between groups were assessed by the Gehan-Breslow-Wilcoxon test.^{15,16} Cox proportional hazards regression model analysis was carried out

to determine potential predictors of OS. *P* values less than .05 were considered significant and are indicated with asterisks. Correlations between the values were analyzed using Pearson's correlation analysis. Statistical analysis was carried out using GraphPad Prism version 6.0 (GraphPad Software) and SPSS version 20.0 (IBM SPSS Statistics).

3 | RESULTS

3.1 | MicroRNA-92b-3p is overexpressed in ccRCC and inversely correlates with patient OS

To confirm the miRNA expression signature of miR-92b-3p in ccRCC, we performed quantitative real-time PCR analysis to compare the expression of miR-92b-3p in ccRCC tissues with normal renal tissues (Table 1). The results indicated that the expression of miR-92b-3p was approximately 2.9-fold higher in the ccRCC tissues than in the adjacent normal renal tissues (Figure 1A), which was consistent with the result of our previous microarray analysis.⁹

In order to evaluate the clinical significance of miR-92b-3p, we tested whether the high expression levels were significantly associated with poor prognosis in ccRCC patients. First, we analyzed an in-house validation cohort of 75 ccRCC patients with surgical management (Table 2). Patients were divided into high- and low-expression groups according to the median expression level of miR-92b-3p. Kaplan-Meier survival analysis revealed that levels of miR-92b-3p were significantly correlated with OS rate (Figure 1B; high vs. low, *P* = .005). Moreover, univariate analysis indicated that OS rate was associated with levels of miR-92b-3p (high vs. low: HR, 2.56; 95% CI, 1.10-5.97; *P* = .030), TNM stage (I, II vs. III, IV: HR, 0.46; 95% CI, 0.21-1.01; *P* = .053), and histopathological nuclear grade (1, 2 vs. 3: HR, 0.43; 95% CI, 0.18-1.00; *P* = .050). Among the parameters above, miR-92b-3p (high vs. low: HR, 2.86; 95% CI, 1.20-6.83; *P* = .018) and TNM stage (I, II vs. III, IV: HR, 0.43; 95% CI, 0.18-0.99; *P* = .048) were significantly associated with patient prognosis when analyzed by multivariate analysis (Table 3).

To further validate the correlation between the miR-92b-3p expression level and OS, we used the SurvMicro tool, which assesses miRNA signatures from publicly available miRNA profiles.¹⁷ We found that miR-92b-3p was also associated with OS in ccRCC patients from TCGA database. (high vs. low: HR, 1.86; 95% CI, 1.21-2.85; *P* = .0044, Figure S1).

Altogether, these data demonstrated that the transcriptional level of miR-92b-3p is upregulated in ccRCC and can be a significant prognostic factor to predict prognosis in ccRCC.

3.2 | Functional analysis of miR-92b-3p

To investigate the role of miR-92b-3p in ccRCC, we first examined the expression levels of miR-92b-3p in RCC cell lines (Caki-1, Caki-2, 786-O, and ACHN cells). Among the 4 cell lines tested, the expression was lowest in ACHN cells, and Caki-2 cells showed the highest expression (Figure 2A). To investigate the potential function of miR-92b-3p, we

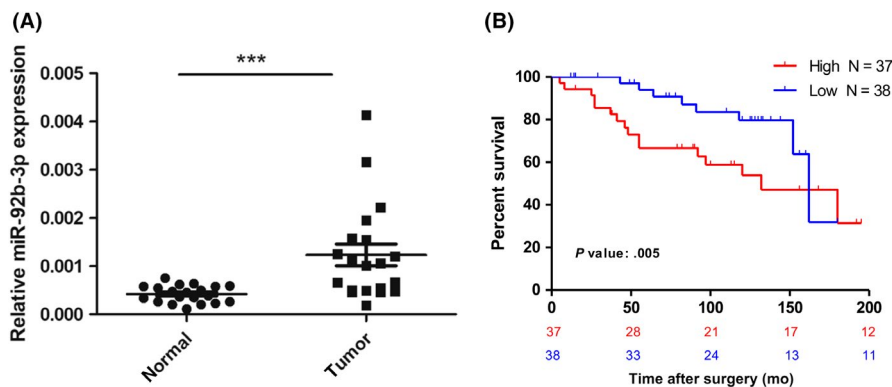


FIGURE 1 MicroRNA (miR)-92b-3p is upregulated in clear cell renal cell carcinoma (ccRCC) and inversely correlates with patient overall survival (OS). A, miR-92b-3p expression in ccRCC tissues. Expression of miR-92b-3p was examined in 20 matched-pair samples of ccRCC by quantitative real-time PCR. Data are the relative expression normalized to U6 snRNA. Comparison was undertaken by Mann-Whitney U test. $***P < .001$. B, Probability estimates of OS of patients. ccRCC samples were divided into 2 groups, high or low levels, based on real-time PCR results. Kaplan-Meier survival estimates stratified by miRNA level. Statistical analysis was carried out using the Gehan-Breslow-Wilcoxon test

	Univariate analysis			Multivariate analysis		
	HR	95% CI	P value	HR	95% CI	P value
Age (<65 vs. ≥ 65 y)	0.76	0.35-1.68	.500	—	—	—
TNM stage (I, II vs. III, IV)	0.46	0.21-1.01	.053	0.43	0.18-0.99	.048
Grade (G1, 2 vs. G3)	0.43	0.18-1.00	.050	0.60	0.24-1.45	.250
Vascular invasion (- vs. +)	0.79	0.31-2.00	.620	—	—	—
Na (<139 vs. ≥ 139) (mEq/L)	0.69	0.27-1.73	.430	—	—	—
NLR (<2.52 vs. ≥ 2.52)	0.79	0.36-1.74	.560	—	—	—
PLR (<1.76 vs. ≥ 1.76)	0.76	0.34-1.70	.500	—	—	—
CRP (<1 mg/dL vs. ≥ 1 mg/dL)	0.77	0.30-1.95	.580	—	—	—
miR-92b-3p (high vs. low)	2.56	1.10-5.97	.030	2.86	1.20-6.83	.018

Abbreviations: CI, confidence interval; CRP, C-reactive protein; HR, hazard ratio; NLR, neutrophil to lymphocyte ratio; PLR, platelet to lymphocyte ratio.

examined the effect of the miR-92b-3p mimic on cell growth, migration, and invasion activities using the ACHN cell line. The miR-92b-3p mimic significantly increased the cell growth ($P < .01$, Figure 2B), migration ($P < .01$, Figure 2C), and invasion ability ($P < .05$, Figure 2D). Next, we examined the effect of a miR-92b-3p inhibitor using the Caki-2 cell line. Although the miR-92b-3p inhibitor had no significant effect on cell migration ($P = .19$, Figure 3A), we observed downregulated proliferation ($P < .01$, Figure 3B) and invasion activity ($P < .05$, Figure 3C) in Caki-2 cells. These results indicate that miR-92b-3p is involved in regulating the expression of crucial molecules in RCC cell lines.

3.3 | TSC1 is a direct target of miR-92b-3p in RCC cells

To identify the potential target of miR-92b-3p, we used the target prediction program miRDB¹⁸ and focused on the *TSC1* gene, an upstream regulator of the mTOR signaling pathway. The target prediction resource MicroRNA.org (<http://www.microRNA.org>) predicted that the 3'-UTR of

TABLE 3 Univariate and multivariate logistic regression analysis on microRNA (miR)-92b-3p expression levels with overall survival in validation cohort (n = 75)

TSC1 mRNA contains a complementary sequence for the seed region of miR-92b-3p (Figure 4A). To confirm whether *TSC1* was a target gene of miR-92b-3p in RCC cells, we cotransfected both miR-92b-3p mimic and luciferase reporter vector containing the predicted miR-92b-3p binding site (within the 3'-UTR of the human *TSC1* gene) in ACHN cells. The luciferase activity of the *TSC1* 3'-UTR construct was significantly reduced upon overexpression of the miR-92b-3p mimic, but not with a negative control mimic (Figure 4B). Conversely, in Caki-2 cells cotransfected with the miR-92b-3p inhibitor, the luciferase activity of the *TSC1* 3'-UTR construct increased when compared to that cotransfected with a negative control inhibitor (Figure 4C). These results indicated that *TSC1* is a direct target of miR-92b-3p in RCC cells.

3.4 | MicroRNA-92b-3p activates mTOR signaling pathway in RCC cells by downregulating TSC1

The miR-92b-3p mimic reduced *TSC1* expression at the protein level in ACHN cells, and the miR-92b-3p inhibitor increased *TSC1*

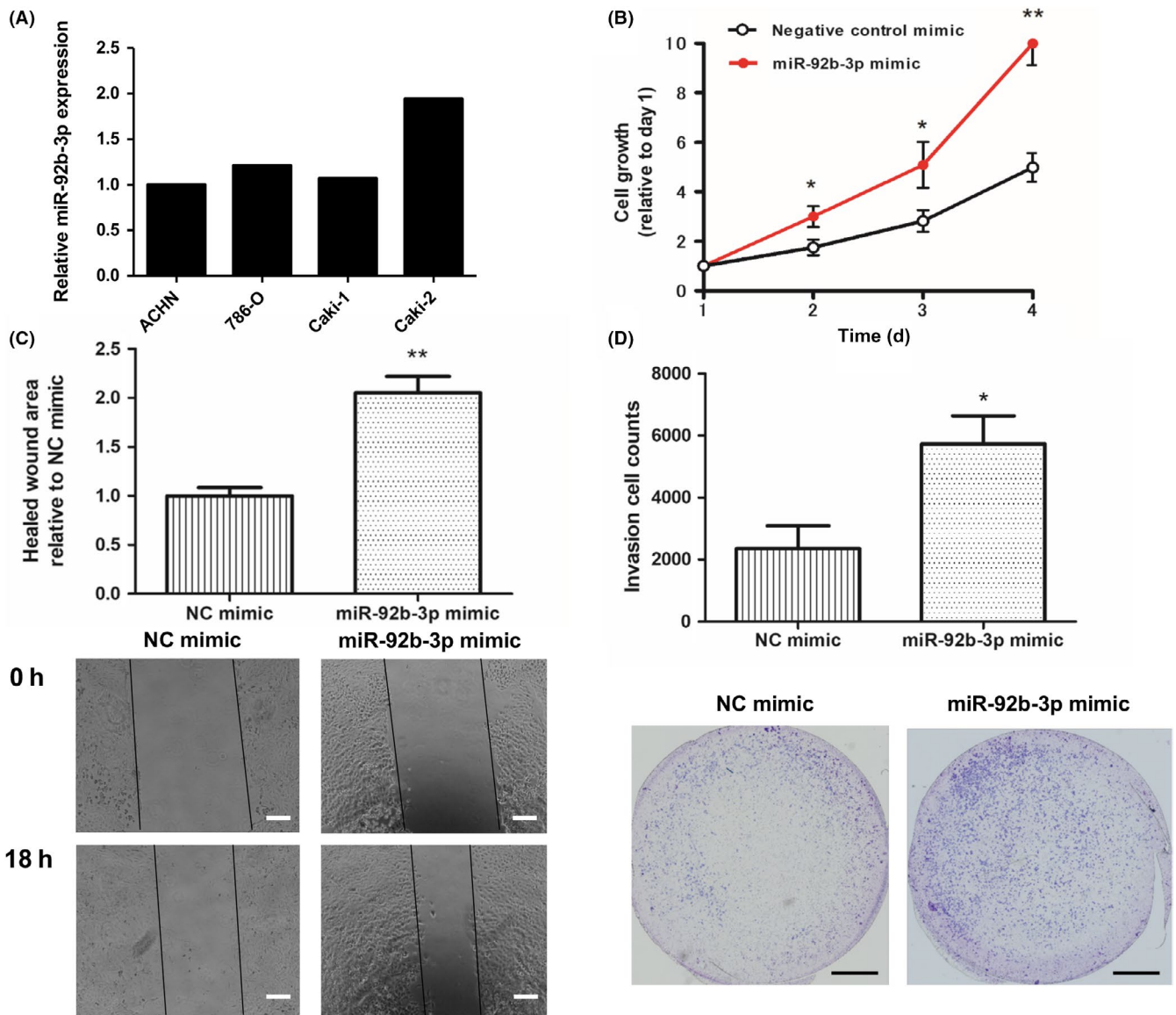


FIGURE 2 MicroRNA (miR)-92b-3p mimic significantly upregulated cell growth, migration, and invasion activities in ACHN cells. A, Expression of miR-92b-3p in 4 renal cell carcinoma (RCC) cell lines was examined by quantitative real-time PCR. B, ACHN cells transfected with miR-92b-3p mimic or negative control (NC) miRNA mimic for 24 h were reseeded in a 96-well plate, incubated for the indicated times, and examined by MTS assay. Values are means \pm SD of 3 independent experiments. * P < .05, ** P < .01 vs. control mimic. C, ACHN cells were transfected with the miR-92b-3p mimic or a negative control miRNA mimic for 72 h. Cell migration was measured 18 h after a wound was created by scraping. Representative results of cell motility in the scratch wound-healing assay are shown. Scale bar = 200 μ m. Results are expressed as mean \pm SD of 3 independent experiments. * P < .05 vs. control mimic. D, ACHN cells were transfected with the miR-92b-3p mimic or a NC miRNA mimic for 72 h. The transfected cell suspension was added to the upper chamber of Matrigel-coated Transwell membrane inserts, and the lower chamber was filled with the complete medium and then cultured for 48 h. Invasive cells that had penetrated the Matrigel membrane were fixed and stained. Scale bar = 1.2 mm. Values are means \pm SD of 3 independent experiments. * P < .05 vs. control mimic

protein expression in Caki-2 cells (Figure 5A). As p70 ribosomal S6 kinase β -1 (S6K) is a downstream factor of TSC1, which drives the oncogenic signaling pathway by upregulating cell growth in RCC cells,¹⁹ we examined the phosphorylation status of S6K. When miR-92b-3p was overexpressed in ACHN cells, phosphorylation of S6K was upregulated. In contrast, inhibition of miR-92b-3p decreased phosphorylation of S6K in Caki-2 cells (Figure 5A). To examine whether the malignant phenotypes upregulated by

the miR-92b-3p in RCC cells were due to the decrease in TSC1 expression, we undertook cell proliferation assays using ACHN cells treated with mTORC1 inhibitor everolimus (RAD001). As expected, the result showed that ACHN cells transfected with miR-92b-3p mimic were more sensitive to everolimus than ACHN cells transfected with negative control mimic (Figure 5B), suggesting that miR-92b-3p upregulates the mTOR signaling pathway by targeting TSC1 in RCC cells. Using TCGA KIRC datasets, we

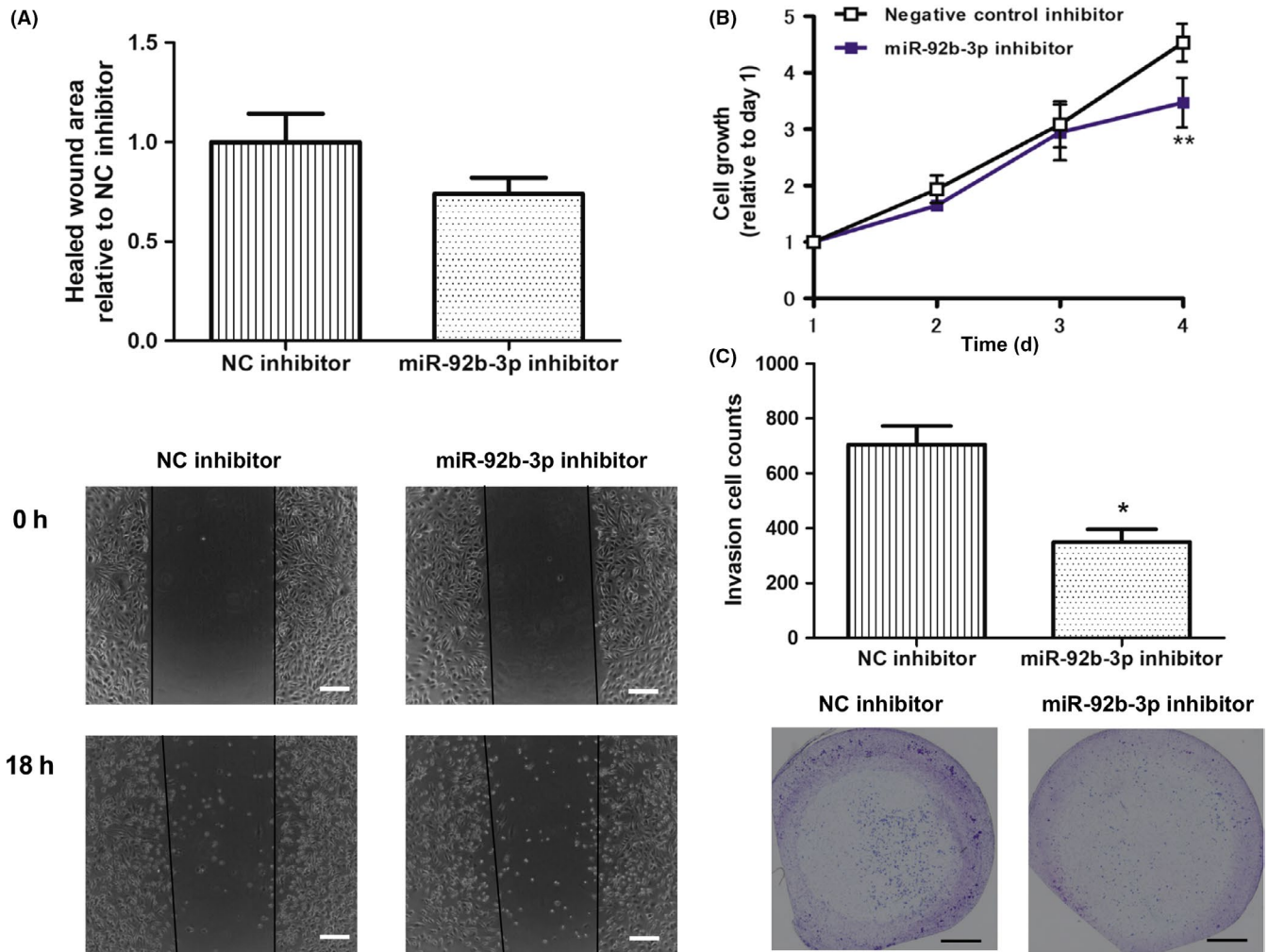


FIGURE 3 MicroRNA (miR)-92b-3p inhibitor downregulated cell growth and invasion activities in Caki-2 cells. A, Caki-2 cells were transfected with the miR-92b-3p inhibitor or a negative control (NC) miRNA inhibitor for 72 h. Cell migration was measured 18 h after a wound was created by scraping. Scale bar = 200 μ m. Results are expressed as mean \pm SD of 3 independent experiments. B, Caki-2 cells transfected with miR-92b-3p inhibitor or NC miRNA inhibitor for 24 h were reseeded in a 96-well plate, incubated for the indicated times, and examined by MTS assay. Values are means \pm SD of 4 independent experiments. ** $P < .01$ vs. control inhibitor. C, Caki-2 cells were transfected with miR-92b-3p inhibitor or NC miRNA inhibitor for 72 h. The transfected cell suspension was added to the upper chamber of Matrigel-coated Transwell membrane inserts, and the lower chamber was filled with the complete medium and then cultured for 48 h. Invasive cells that had penetrated the Matrigel membrane were fixed and stained. Scale bar = 1.2 mm. Values are means \pm SD of 3 independent experiments. * $P < .05$ vs. control mimic

also clarified that both the mRNA expression levels ($\rho = -0.26$, $P < .001$, Fig. S2), and the protein expression levels ($\rho = -0.22$, $P = .001$, Figure S3) of TSC1 showed a weak negative correlation with miR-92b-3p expression in the ccRCC samples. Moreover, low protein levels of TSC1 were significantly associated with poor prognosis in ccRCC patients (Figure S4). To further examine the protein levels of TSC1 in ccRCC and normal tissues, 30 formalin-fixed paraffin-embedded clinical specimens from ccRCC patients were immunohistochemically stained with an anti-TSC1 Ab. The levels of TSC1 staining were classified as medium and low (staining score, 1-2; Figure 5C). TSC1 was moderately stained and evenly distributed in the cytosol of normal renal tissues, but weakly stained in the ccRCC tissues (Figure 5C). These results are consistent with the upregulated expression levels of miR-92b-3p

observed in ccRCC tissues compared with paired normal tissues (Figure 1A).

4 | DISCUSSION

There have been several reports showing that miR-92b-3p functions as an oncomiR in several types of cancer.^{10,11} Wu et al reported that miR-92b-3p functions as a potential oncogenic miRNA in glioblastomas by targeting *SMAD3*.²⁰ In nonsmall-cell lung cancer, miR-92b-3p directly targets *PTEN*, promotes cell growth, and induces cisplatin chemosensitivity.²¹ However, miR-92b-3p has also been reported to act as a tumor suppressor miRNA.¹² The present study shows for the first time that miR-92b-3p functions as an oncomiR in both RCC cell

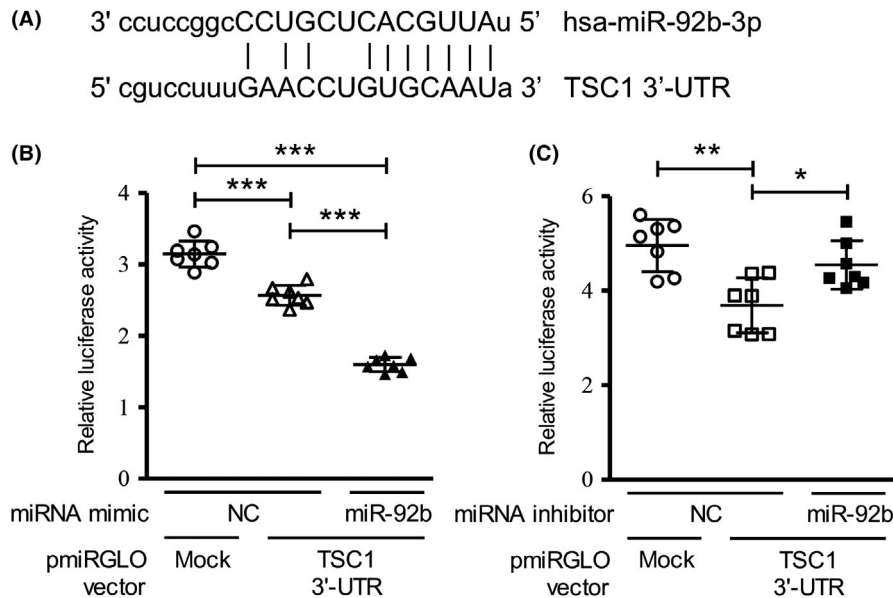


FIGURE 4 MicroRNA (miR)-92b-3p targets *TSC1* in renal cell carcinoma (RCC) cells. A, Predicted miR-92b-3p-binding site within the 3'-UTR of the human *TSC1* gene. B, ACHN cells were cotransfected with the luciferase reporter construct containing the predicted miR-92b-3p-binding site within the *TSC1* 3'-UTR and miR-92b-3p mimic, or a negative control (NC) miRNA mimic. C, Caki-2 cells were cotransfected with the luciferase reporter construct containing the predicted miR-92b-binding site in the *TSC1* 3'-UTR and miR-92b inhibitor, or NC miRNA inhibitor. Relative luciferase activities were calculated as ratios of firefly luminescence / *Renilla* luminescence. Values presented as mean \pm SD of 7 independent experiments (B,C). One-way ANOVA with Tukey's post hoc tests. * $P < .05$, ** $P < .01$, *** $P < .001$

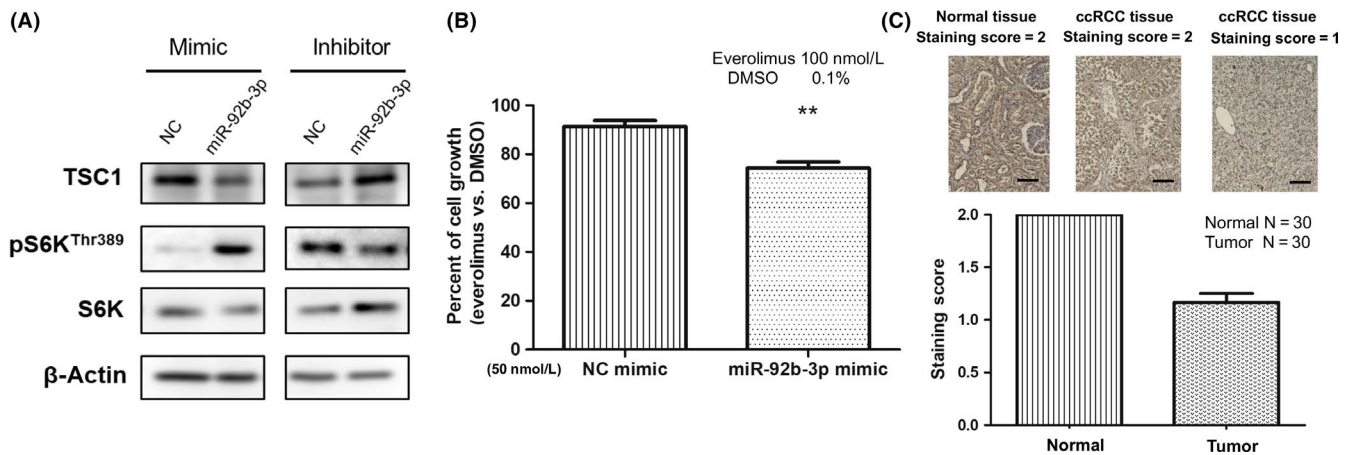


FIGURE 5 MicroRNA (miR)-92b-3p regulates the mTOR signaling pathway by targeting *TSC1*, and *TSC1* is downregulated in clear cell renal cell carcinoma (ccRCC) specimens compared to adjacent normal tissues. A, Representative images of western blot analysis from 3 independent experiments showing the protein levels of *TSC1* and *p70S6K(Thr389)* and *S6K* in ACHN cells transfected with miR-92b-3p mimic, or a negative control (NC) miRNA mimic, and also in Caki-2 cells transfected with miR-92b-3p inhibitor, or NC miRNA inhibitor. B, Proliferation assay of ACHN cells transfected with a miR-92b-3p mimic or NC mimic after 96 h incubation with either everolimus or vehicle control (0.1% DMSO). Values are means \pm SD of 3 independent experiments. Comparison was carried out by unpaired Student's *t* test. ** $P < .01$. C, Representative images of immunohistochemical staining for *TSC1* in ccRCC tissues and normal tissues. Paired tissues (30 samples of each) were examined and *TSC1* staining intensity was classified into 2 levels: weak = 1 and moderate = 2. Mean scores of normal tissues and ccRCC tissues are shown in the bar graph. Scale bar = 100 μ m

lines and ccRCC clinical specimens. Importantly, based on both TCGA database and our in-house data analysis, we found that miR-92b-3p expression displays a significant inverse correlation with ccRCC patient OS, nominating miR-92b-3p as a prognostic miRNA in ccRCC.

The *TSC1/TSC2* complex functions as a tumor suppressor by inhibition of the downstream mTOR signaling pathway, which

regulates cell size and proliferation by promoting translation activity.¹⁹ A recent study showed that in a kidney-specific *TSC1* inactivation mouse model, the mice developed progressive RCC due to chronic mTORC1 upregulation and subsequent accumulation of the oncometabolite fumarate.²² Thus, the *TSC1*-mTOR axis is important in ccRCC development. There is accumulating

evidence for miRNA-mediated regulation of the mTOR signaling pathway in different cancer types.²³ However, to our knowledge, there are no miRNAs that have been reported to be associated with the regulation of mTOR signaling in RCC. In the present study, we identified miR-92b-3p as a suppressor of *TSC1* expression and an activator of the mTOR signaling pathway by upregulating phosphorylated S6K levels in RCC cells. Furthermore, we found *TSC1* protein expression was downregulated in ccRCC tissues when compared with paired normal renal tissues. The *TSC1* gene was previously reported to be mutated in only approximately 4% of ccRCC, and no correlations were found between mutations and mTORC activation in tumors.²⁴ Given the low frequency of *TSC1* mutations in ccRCC, other mechanisms might exist to account for the relative low protein expression of *TSC1* in ccRCC tumor tissues compared to normal counterparts. Based on our results (Figures S2 and S3), we hypothesized that the relatively high miR-92b-3p expression in ccRCC tissues could correlate with the reduced protein expression of *TSC1* in ccRCC.

There are some limitations in the present study. Although we have shown that miR-92b-3p regulated not only cell growth (Figures 2, 2 and S5), but also cell invasion in RCC cells (Figures 2 and 2), it is not clear whether the described cellular phenotypic changes were caused directly by the variation in *TSC1* expression. To our knowledge, the *TSC1*-mTOR signaling pathway plays important roles in the regulation of cell growth and proliferation, but little is known about the regulation of cell invasion activities. It should also be noted that the target prediction programs predicted miR-92b-3p-putative binding sequences in other genes involved in the invasion in RCC: *PTE*²⁵ and Dickkopf-related protein-3 (*DKK-3*).²⁶ As a single miRNA can regulate multiple protein-coding and noncoding RNA transcripts in cells, miR-92b-3p could also mediate RCC cell invasion activities through other target molecules. In addition, it is also necessary to use mouse models to further evaluate the potential of miR-92b-3p for miRNA therapeutics.

Taken together, our study indicates that miR-92b-3p plays an important role in ccRCC progression and predicts poor patient OS. In the future, miR-92b-3p could be a potential target for RCC treatment.

ACKNOWLEDGMENTS

This study was supported by JSPS KAKENHI (Grant-in-Aid for Research Activity start-up, grant no. A16H069540).

CONFLICT OF INTEREST

The authors have no conflicts of interest.

ORCID

Cong Wang  <https://orcid.org/0000-0001-8445-6205>

Yujiro Hayashi  <https://orcid.org/0000-0002-4701-5635>

Taigo Kato  <https://orcid.org/0000-0002-8681-1407>

Atsunari Kawashima  <https://orcid.org/0000-0001-9369-4264>

REFERENCES

1. Marumo K, Kanayama H, Miyao N, et al. Prevalence of renal cell carcinoma: a nation-wide survey in Japan in 2002. *Int J Urology*. 2007;14:479-482.
2. Nerich V, Hugues M, Paillard MJ, et al. Clinical impact of targeted therapies in patients with metastatic clear-cell renal cell carcinoma. *Onco Targets Ther*. 2014;7:365-374.
3. Ha M, Kim VN. Regulation of microRNA biogenesis. *Nat Rev Mol Cell Biol*. 2014;15:509-524.
4. Jansson MD, Lund AH. MicroRNA and cancer. *Mol Oncol*. 2012;6:590-610.
5. Lin S, Gregory RI. MicroRNA biogenesis pathways in cancer. *Nat Rev Cancer*. 2015;15:321-333.
6. Li M, Wang Y, Song Y, et al. MicroRNAs in renal cell carcinoma: a systematic review of clinical implications. *Oncol Rep*. 2015;33:1571-1578.
7. Jingushi K, Ueda Y, Kitae K, et al. miR-629 Targets TRIM33 to Promote TGF β /Smad Signaling and Metastatic Phenotypes in ccRCC. *Mol Cancer Res*. 2015;3:565-574.
8. Jingushi K, Kashiwagi Y, Ueda Y, et al. High miR-122 expression promotes malignant phenotypes in ccRCC by targeting occludin. *Int J Oncol*. 2017;1:289-297.
9. Nakata W, Uemura M, Sato M, et al. Expression of miR-27a-3p is an independent predictive factor for recurrence in clear cell renal cell carcinoma. *Oncotarget*. 2015;25:21645-21654.
10. Gong L, Ren MY, Lv ZB, Yang YL, Wang ZW. miR-92b-3p promotes colorectal carcinoma cell proliferation, invasion, and migration by inhibiting FBXW7 in vitro and in vivo. *DNA Cell Biol*. 2018;37:501-511.
11. Omura T, Shimada Y, Nagata T, et al. Relapse-associated microRNA in gastric cancer patients after S-1 adjuvant chemotherapy. *Oncol Rep*. 2014;31:613-618.
12. Long NM, Zhan M, Xu SW, et al. miR-92b-3p acts as a tumor suppressor by targeting Gabra3 in pancreatic cancer. *Mol Cancer*. 2017;16:167.
13. Greene FL, Page DL, Fleming ID, et al. Staging manual. *Ann Oncol*. 2003;14:345-346.
14. Mostofi FK. *International Histological Classification of Tumors No. 25: Histological Typing of Kidney Tumors*. New York, NY:Springer;1981.
15. Breslow NE. A generalized Kruskal-Wallis test for comparing K samples subject to unequal patterns of censorship. *Biometrika*. 1970;57:579-594.
16. Gehan EA. A generalized Wilcoxon test for comparing arbitrarily single-censored samples. *Biometrika*. 1965;52:203-223.
17. Acuirre-Gamboa R, Trevino V. SurvMicro: assessment of miRNA-based prognostic signatures for cancer clinical outcomes by multivariate survival analysis. *Bioinformatics*. 2014;11:1630-1632.
18. Nathan W, Xiaowei W. miRDB: an online resource for microRNA target prediction and functional annotations. *Nucleic Acids Res*. 2015;43:146-152.
19. Huang J, Manning BD. A complex interplay between Akt, TSC2 and the two mTOR complexes. *Biochem Soc Trans*. 2009;37:217-222.
20. Wu ZB, Cai L, Lin SJ, et al. The miR-92b functions as a potential oncogene by targeting on Smad3 in glioblastomas. *Brain Res*. 2013;1529:16-25.
21. Li Y, Li L, Guan Y, et al. MiR-92b regulates the cell growth, cisplatin chemosensitivity of U2OS non small cell lung cancer cell line and target PTEN. *Biochem Biophys Res Commun*. 2013;440:604-610.
22. Drusian L, Nigro EA, Mannella V, et al. mTORC1 upregulation leads to accumulation of the oncometabolite fumarate in a mouse model of renal cell carcinoma. *Cell Rep*. 2018;24:1093-1104.
23. Zhang Y, Huang B, Wang HY, et al. Emerging role of microRNAs in mTOR signaling. *Cell Mol life Sci*. 2017;74:2613-2625.

24. Kucejova B, Pena-Llopis S, Yamasaki T, et al. Interplay between pVHL and mTORC1 pathways in clear-cell renal carcinoma. *Mol Cancer Res*. 2011;9:1255-1265.
25. Ma Q, Peng ZQ, Wang L, et al. miR-19a correlates with poor prognosis of clear cell renal cell carcinoma patients via promoting cell proliferation and suppressing PTEN/SMAD4 expression. *Int J Oncol*. 2016;6:2589-2599.
26. Zhang XL, Xu G, Zhou Y, Yan JJ. MicroRNA-183 promotes the proliferation and metastasis of renal cell carcinoma through targeting Dickkopf-related protein 3. *Oncology Letters*. 2018;3(4): 6003-6008.

SUPPORTING INFORMATION

Additional supporting information may be found online in the Supporting Information section.

How to cite this article: Wang C, Uemura M, Tomiyama E, et al. MicroRNA-92b-3p is a prognostic oncomiR that targets *TSC1* in clear cell renal cell carcinoma. *Cancer Sci*. 2020;111: 1146-1155. <https://doi.org/10.1111/cas.14325>